

Resolving Non-Gaussian Diffusion in Mouse Trigeminal Nerve using both Diffusion Kurtosis Imaging (DKI) and Diffusion Basis Spectrum Imaging (DBSI)

Yong Wang¹, Els Fieremans², Peng Sun¹, and Sheng-Kwei Song¹

¹Radiology, Washington University in St. Louis, Saint Louis, MO, United States, ²Radiology, New York University, New York, NY, United States

Introduction:

Although diffusion tensor imaging (DTI) has been successfully used to measure the apparent directional diffusivity and detect axonal/myelin dysfunction in white matter injury (1), its hidden assumption of Gaussian diffusion hampered its application to quantify non-Gaussianity caused by the boundary restriction effect and the presence of multiple diffusion compartments with distinct diffusivities. Many new diffusion MRI techniques have been proposed to model the non-Gaussian diffusion over the last decade, such as generalized DTI (gDTI), diffusion spectrum imaging (DSI), diffusion kurtosis imaging (DKI), composite hindered and restricted model of diffusion (CHARMED) etc. Most recently, an idealized two-compartment no exchange diffusion model of white matter was proposed (2) that allows estimation of the intra- and extra-axonal diffusivities, as well as the intra-axonal water fraction from the clinically feasible DKI-indices. Based on a multiple tensor model, we have recently developed a new diffusion MRI method, diffusion basis spectrum imaging (DBSI), to quantify crossing fibers and partial volume effect of inflammatory response (3). In the present study, an intra-axonal water diffusion component is further included in DBSI method to model the non-Gaussian restricted anisotropic diffusion inside axons. Normal mouse trigeminal nerves were examined using a spin-echo diffusion weighted spectroscopy (MRS) sequence, and the data were analyzed to estimate the intra-axonal water fraction and associated indices using both DKI and DBSI. The preliminary data support the agreement between DBSI and DKI.

Method:

Animal Model: Five trigeminal nerves from 5 normal male C57BL/6 mice (The Jackson Laboratory, Bar Harbor, ME) were isolated after fixation. **MR:** Diffusion MRS of the trigeminal nerve was performed using an Agilent DirectDrive console equipped with a 4.7 T magnet. 99 distinct diffusion-weighting gradients on a 3D grid were employed (3). Maximal diffusion weighting $b = 3200$ (s/mm²). TR= 2s, TE=48.8ms, $\Delta = 24$ ms, $\delta=8$ ms. The scan time was 198 seconds.

DKI Analysis: The diffusion and kurtosis tensor were calculated from the diffusion weighted signals with a weighted constrained linear least squares fitting algorithm (4), and then used to derive the intra-axonal water fraction, and the compartmental diffusion tensors for the intra-/extra-axonal space (2).

DBSI Analysis: The detailed description of DBSI can be found in a recent publication (3). Briefly, Eq. [1] was solved by fitting the 99 diffusion weighted signals using a linear combination of diffusion basis sets consisting of cylindrically symmetric diffusion tensors (3) with the freedom to vary $\lambda_{||}$ and λ_{\perp} to estimate the number of anisotropic diffusion tensor components (N_{aniso}) and the associated principal directions. After N_{aniso} was computed, the number of isotropic component (N_{iso}) was further determined using nonnegative least-squares (NNLS) analysis (3). The global nonlinear optimization was conducted employing direct pattern search to solve Eq. [1]. S_k is the k th measured diffusion weighted signals ($k = 1, 2, 3, \dots, 99$). S_i and S_j are fractions of anisotropic diffusion components and isotropic diffusion component respectively.

Intra-axonal Water Diffusion: As suggested previously (2), the axon diameter can be approximately treated as zero under the assumption of long diffusion time. For the coherent mouse trigeminal nerve, an anisotropic diffusion component with radial diffusivity equal to zero is included in Eq. [2]. For coherent trigeminal nerve ($N_{aniso}=1$), Eq. [2] is solved by fitting the measured 99 mouse trigeminal nerve diffusion weighted signals using global nonlinear optimization and NNLS analysis (3). \tilde{S} and $\bar{\lambda}_{||}$ are the anisotropic intra-axonal water fraction and axial diffusivity. $\tilde{S}, \bar{\lambda}_{||}, \bar{\lambda}_{\perp}$ are the anisotropic extra-axonal water fraction and axial/radial diffusivities. The restricted isotropic components with mean ADC close to zero were assigned to cells, while the rest of the isotropic components were assigned to isotropic extra-axonal water (1). In order to compare with the DKI-derived indices (based on only two compartments), DBSI derived anisotropic intra-axonal diffusion was combined with restricted isotropic diffusion (cells) as DBSI derived intra-cellular diffusion. Similarly, DBSI derived anisotropic extra-axonal diffusion was combined with isotropic extra-axonal diffusion as DBSI derived extra-cellular diffusion.

Results and Discussion:

The Bland-Altman plots for the DBSI and DKI derived intra-axonal water fraction (Panel A), intra-axonal axial diffusivity (Panel B), extra-axonal axial (Panel C) and radial diffusivity (Panel D) are shown in Figure 1. The detailed numbers of these parameters were listed in Table 1, as well as the restricted isotropic component, that is uniquely derived with DBSI and correlates well with the cellularity extent (3). Our results demonstrate that DBSI and DKI, both non-Gaussian diffusion methods based on relatively low b diffusion measurements and similar assumptions, yield realistic values for the intra-axonal water fraction and the compartment diffusivities. While the advantage of DKI is a straightforward linear fitting procedure, DBSI provides additional microstructural parameters that may serve as useful biomarkers in neuropathologies.

Table 1: DBSI and DKI derived indices. Diffusivity is in $\mu\text{m}^2/\text{ms}$

Trigeminal Nerve (TN)	DBSI Intra-cellular Water Fraction	DKI Intra-axonal Water Fraction	DBSI Intra-cellular Axial Diffusivity	DKI Intra-axonal Axial Diffusivity	DBSI Extra-cellular Axial Diffusivity	DKI Extra-axonal Axial Diffusivity	DBSI Extra-cellular Radial Diffusivity	DKI Extra-axonal Radial Diffusivity	DBSI Cell Fraction
TN1	0.38	0.31	0.57	0.67	1.30	1.13	0.49	0.41	0.05
TN2	0.35	0.30	0.54	0.65	1.25	1.12	0.49	0.44	0.06
TN3	0.40	0.30	0.54	0.63	1.24	1.08	0.55	0.44	0.06
TN4	0.39	0.30	0.55	0.61	1.17	1.07	0.51	0.40	0.06
TN5	0.39	0.30	0.58	0.63	1.23	1.13	0.56	0.43	0.07

References: (1) Song, SK. et al. *Neuroimage*. 2002; 17:1429. (2) Fieremans, E. et al. *Neuroimage*. 2011; 58:177-188. (3) Wang, Y. et al. *Brain*. 2011. In Press.; (4) Tabesh, A. et al. *MRM*. 2011; 65:823-836

$$S_k = \sum_{i=1}^{N_{aniso}} S_i e^{-\frac{b}{\lambda_{||}} \left| \frac{\lambda_{\perp}}{e} \right| \left| \frac{b}{\lambda_{||}} \right| (\lambda_{||} - \lambda_{\perp}) \cos^2 \theta_i} + \sum_{j=1}^{N_{iso}} S_j e^{-\frac{b}{\lambda_{||}} \left| \frac{b}{\lambda_{||}} \right| d_j} \quad [1]$$

$$S_k = \tilde{S} e^{-\frac{b}{\lambda_{||}} \left| \frac{\lambda_{\perp}}{e} \right| \left| \frac{b}{\lambda_{||}} \right| (\tilde{\lambda}_{||} - \tilde{\lambda}_{\perp}) \cos^2 \theta} + \bar{S} e^{-\frac{b}{\lambda_{||}} \left| \frac{b}{\lambda_{||}} \right| \bar{\lambda}_{||} \cos^2 \theta} + \sum_{j=1}^{N_{iso}} S_j e^{-\frac{b}{\lambda_{||}} \left| \frac{b}{\lambda_{||}} \right| d_j} \quad [2]$$

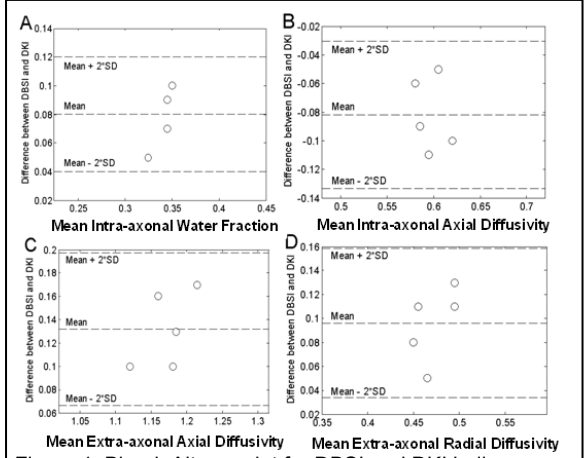


Figure 1. Bland-Altman plot for DBSI and DKI indices.